order transverse mode is shown to operate up to an output power of greater than 180 mW CW. The lateral divergence is 10° full width at half maximum (FWHM). The divergence perpendicular to the *p–n* junction is approximately 35° FWHM.

The spectral output of the single stripe laser is presented in Fig. 3. The laser operates in a single longitudinal mode up to

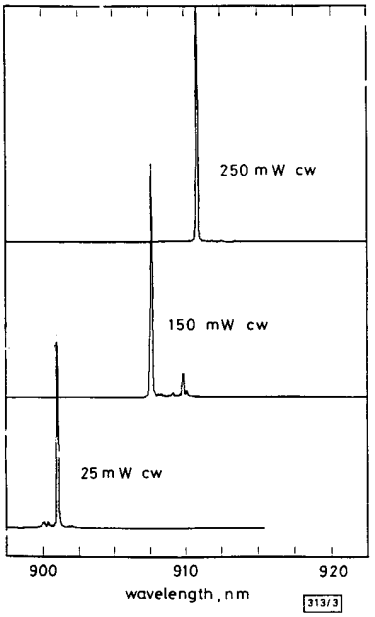

Fig. 3 *Spectral output from single stripe InGaAs/AlGaAs laser diode*

operating ranges of 180 mW CW where the laser deviates from the lowest order transverse mode. In addition there are regions of operation where a single transverse mode is maintained at even higher output power levels. The highest output power at which single longitudinal mode operation was achieved was 250 mW CW. This seems to correspond to the region where the light output becomes sublinear with input current. The emission wavelength is near 910 nm.

In conclusion, 4 μm wide single stripe laser diodes have been fabricated from pseudomorphic, InGaAs/AlGaAs, epitaxial material. The diodes operate at powers exceeding 350 mW CW, while maintaining a single transverse and longitudinal mode up to power outputs of 180 mW CW. The spectral output is near 910 nm. Such a source may be useful for creating efficient blue light at 455 nm via frequency doubling.[10–12]

The authors would like to thank Ross Parke, Paul Tally, Tim Earls, Toni Tally, David Mehuys, Rob Waarts and Sean Ogarrio for their support.

D. F. WELCH
M. CARDINAL
B. STREIFER
D. SCIFRES

Spectra Diode Laboratories
80 Rose Orchard Way
San Jose, CA 95134, USA

24th November 1989

References

1 WELCH, D. F., STREIFER, W., and SCIFRES, D. R.: 'High power single mode laser diodes'. SPIE Laser Diode Technology and Applications, 1989, **1043**, pp. 54–60
2 SDL-5410 commercially available 100 mW CW, single mode laser
3 WELCH, D. F., SCHAUS, C. F., SUN, S., GOURLEY, P. L., and STREIFER, W.: 'Gain characteristics of strained quantum well lasers', to be published in *Appl. Phys. Letts.*
4 YABLONOVITCH, E., and KANE, E. O.: 'Band structure engineering of semiconductor lasers for optical communications', *J. Lightwave Tech.*, 1988, **6**, (8), pp. 1292–1299
5 MAJOR, J. S., GUIDO, L. J., HSIEH, K. C., HOLONYAK, N., STUTIUS, W., GAVRILOVIC, P., and WILLIAMS, J. E.: 'Low-threshold disorder defined buried heterostructure strained layer AlGaAs/GaAs/InGaAs quantum well lasers', *Appl. Phys. Letts.*, 1989, **54**, (10), pp. 913–915
6 YORK, P. K., BEERNINK, K. J., FERNANDEZ, G. E., and COLEMAN, J. J.: 'InGaAs–GaAs strained layer quantum well buried heterostructure lasers by metalorganic chemical vapour deposition', *Appl. Phys. Lett.*, 1989, **54**, (6), pp. 499–501
7 TSANG, W. T.: 'Extension of lasing wavelengths beyond 0·87 μm in GaAs/AlGaAs double heterostructure lasers by In incorporation in the GaAs active layers during molecular beam epitaxy', *Appl. Phys. Lett.*, 1981, **38**, (9), pp. 661–663
8 BOUR, D. P., MARTINELLI, R. U., GILBERT, D. B., ELBAUM, L., and HARVEY, M. G.: 'Operating characteristics of InGaAs/AlGaAs strained single quantum well lasers', *Appl. Phys. Letts.*, 1989, **55**, (15), pp. 1501–1503
9 STUTIUS, W., GAVRILOVIC, P., WILLIAMS, J. E., MEEHAN, K., and ZARRABI, J. H.: 'Continuous operation of high power strained layer GaInAs/AlGaAs quantum well lasers', *Electron. Lett.*, 1988, **24**, (24), pp. 1493–1494
10 GOLDBERG, L., and CHUN, M.: 'Efficient generation of 421 nm by resonantly enhanced doubling of GaAlAs laser diode array emission', *Appl. Phys. Lett.*, 1989, **55**, (3), pp. 218–221
11 KOZLOVSKY, W., NABORS, C. D., and BYER, R. L.: 'Efficient second harmonic generation of a diode laser pumped cw Nd : YAG laser using monolithic MgO : $LiNbO_3$ external resonant cavities', *J. Quant. Electr.*, 1988, **24**, (6), pp. 913–919
12 BAER, T., DEIRSTEAD, M. S., and WELCH, D. F.: 'Efficient frequency doubling of a diode laser'. Conference on Lasers and Electro-optics, 1989

COMPARISON OF THREE NUMERICAL TREATMENTS FOR THE OPEN-ENDED COAXIAL LINE SENSOR

Indexing terms: Microwave circuits and systems, Numerical methods and number theory, Microwave measurements

The open-ended coaxial line sensor is commonly used for non-invasive microwave dielectric measurements. A comparison is made between three mathematical treatments that allow the reflection coefficient of the sensor to be derived from the complex permittivity of the material with which it is in contact. It is shown that the discrepancies between values computed by the three methods are much smaller than the predicted measurement uncertainties. Mappings of permittivity contours onto the complex reflection coefficient plane are shown.

The open-ended coaxial line sensor, shown in Fig. 1, is commonly used with automated network analysers and other reflectometers for non-invasive measurement of the complex permittivity of materials at radio and microwave frequencies. Equivalent circuits are often used to model the relationship between the relative permittivity ε^* of the material and the measured reflection coefficient Γ^* of the sensor in contact with the material, where $\varepsilon^* = \varepsilon' - j\varepsilon''$ and $\Gamma^* = \Gamma \exp(j\theta)$. However, it has been argued that if numerical analysis is employed instead of an equivalent circuit treatment, a wider range of permittivity values can be determined more accurately with a particular sensor over a given frequency range,[1] a conclusion that was reached on the basis of only a single

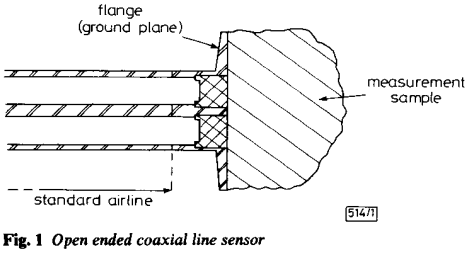

Fig. 1 *Open ended coaxial line sensor*

numerical method. To improve confidence in such methods, it is desirable to compare a number of them and to show that the discrepancies between computed values are insignificant in comparison with the predicted measurement uncertainties. To this end, a comparison of three treatments is now presented. These are based upon point matching,[1,2] the method of Nevels *et al.*[3,4] and a variational method.[5] Each has been programmed independently by a different numerical analyst.

Each of the methods relies on a number of simplifying assumptions:

(*a*) The measurement configuration is completely axisymmetric.

(*b*) The diameter of the ground plane is large in comparison with the diameter of the coaxial line and can be considered to be infinite.

(*c*) The frequency of the radiation in the line is such that only the lowest mode, the TEM mode, is propagated (although TM_{0n} evanescent modes generated at the ground plane discontinuity are taken into account).

Two of the treatments assume that the dielectric material occupies the entire half-space adjacent to the ground plane, while Nevels's technique[3] has been adapted to treat also the case of a dielectric material of finite thickness, backed by an infinite, perfectly conducting sheet parallel to the ground plane.[4] Dielectric specimens of effectively 'infinite thickness' are easily treated as a special case of this configuration, so that direct comparison with the other two programs is possible.

The natural co-ordinates for the configuration are cylindrical polar co-ordinates, with r representing the radial distance from the axis, ϕ the angular measure around the axis and z the displacement along the axis. The electric and magnetic fields in the coaxial line and the half space can be expressed in terms of E_r, E_z and H_ϕ, which are the components of a combined TEM and TM_{0n} electromagnetic field. The boundary conditions at the interface plane between the line and the half-space require E_r and H_ϕ to be continuous across the plane. In all three methods, E_r is taken as fundamental and H_ϕ is deduced from it. In the method due to Nevels *et al.*, rE_r is approximated by a set of 'top-hat' elements whose heights are the parameters to be determined. In the other two methods, E_r is represented as a sum over a finite number of modes in the line and the proportions of the modes in the sum are taken as parameters. The introduction of these parameters makes E_r automatically continuous across the interface for each method. The requirement for H_ϕ to be continuous then becomes a linear integral equation; the parameters are extracted by a technique consistent with the particular method used to make E_r discrete. In the point-matching method and the method of Nevels *et al.*, the values of H_ϕ at an infinitesimal distance each side of the interface are directly equated at a number of particular radii. In the case of the variational method, the integral equation for H_ϕ is itself integrated with respect to each of the modes used in the sum approximation for E_r, making use of the orthogonality properties of these modes.

Of necessity, only a limited number n of modes or radii may be used to approximate the fields. For each of the methods, the result Γ^*_∞ for $n = \infty$ is estimated by quadratic extrapolation from the results for, say, $n = 4$, 8 and 16; results for finite n are assumed to be of the form $(\Gamma^*_n = \Gamma^*_\infty + a/n + b/n^2)$, where a and b are constants. Fig. 2 shows the intermediate and extrapolated results from each of the three programs for one hypothetical measurement configuration. In each case, Γ^* has been calculated at 1 GHz for an open ended coaxial line sensor with inner- and outer-conductor radii of 2·333 mm and 7·549 mm, respectively, containing a dielectric for which $\varepsilon' = 2{\cdot}15$. The sensor is assumed to be placed in contact with an infinite dielectric specimen for which $\varepsilon^* = (100 - j100)$. The maximum discrepancies between extrapolated values are 0·0001 in Γ (amplitude) and 0·014° in θ (phase) for this example. In comparison, the very best attainable measurement uncertainties at this frequency are estimated to be of the order of 0·001 in Γ and 0·3° in θ, and the computational discrepancies are therefore relatively insignificant. It is interesting to note that although variational methods are often considered to be superior to other discrete methods, this theoretical superiority has not been detected in the present work.

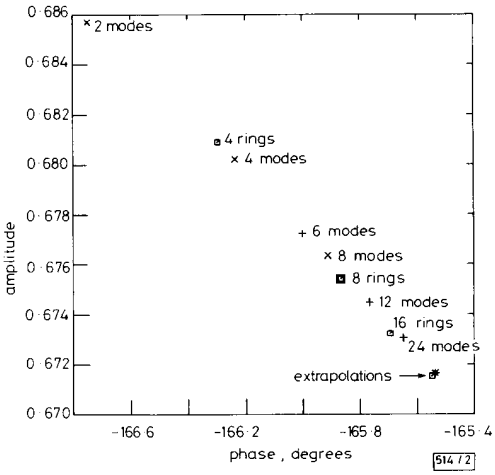

Fig. 2 *Comparison of results at 1 GHz for $\varepsilon^* = (100 - j100)$*
× variational; + point matching; ⊡ Nevels *et al.*

Fig. 3 shows the extrapolated results from the three programs for methanol computed at 15 frequencies between 200 MHz and 3 GHz for the same sensor. The values of ε' and ε'' at each frequency have been calculated from the Cole–Cole parameters derived by Jordan *et al.*[6] by frequency domain measurements. Predicted measurement uncertainties for the coaxial line sensor are indicated for three data points, and it is seen that these are again much greater than the discrepancies between the results from the three programs.

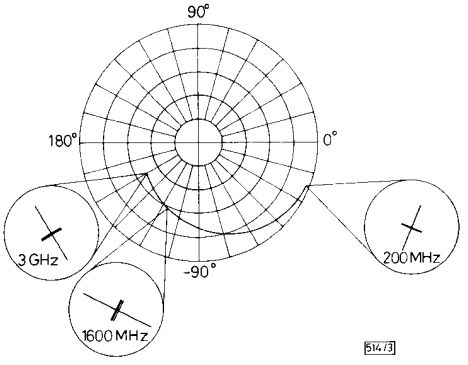

Fig. 3 *Extrapolated results for methanol at 25°C between 200 MHz and 3 GHz using the three methods, with predicted measurement uncertainties*
The three expanded regions have been magnified by a factor of 100

In practical applications, Γ^* is the measured parameter and ε^* must be computed. This 'inverse' calculation is performed by a Newton–Raphson iteration of the 'forward' algorithm, from an initial estimate of ε^*.[1] The estimated uncertainties in computed values of ε' and ε'' depend not only on the uncertainties in Γ and θ at the measurement frequency, but also on the partial derivatives of ε' and ε'' with respect to Γ and θ, which vary as Γ and θ vary. Figs. 4*a* and *b* show how contours of ε' and ε'' map on to the polar chart of Γ^* for the sensor at two different frequencies. The regions of good measurement resolution correspond to well spaced contours, where the partial derivatives are small and errors in the mea-

sured Γ^* will lead to relatively small errors in ε^*. Conversely, regions of poor resolution correspond to closely packed contours.

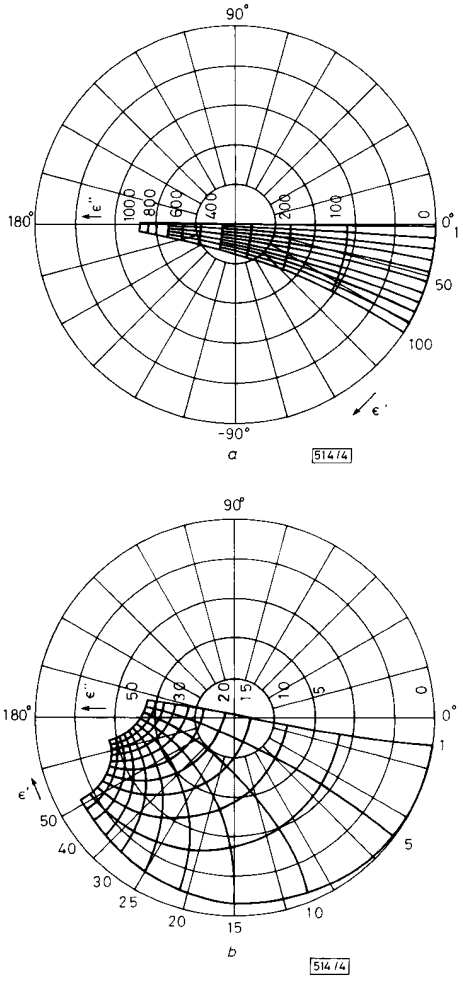

Fig. 4 *Mappings of ε^* onto polar chart of Γ^**
a 100 MHz; *b* 2 GHz

Three other features of the mappings that have a bearing upon approximating equivalent circuits may be noted from Fig. 4*b*. First, the amplitude of the reflection coefficient is less than 1·0 for a lossless dielectric ($\varepsilon'' = 0{\cdot}0$) because of radiative power loss into the half-space. Secondly, the contours for high ε' and high ε'' extend well into the inductive half of the reflection coefficient chart, indicating that equivalent circuit approximations for open-ended coaxial line sensors should contain at least one inductive component. Thirdly, a close inspection of the $\varepsilon' = 1{\cdot}0$ contour shows that it has a double curvature. This is not consistent with a simple equivalent circuit containing only one permittivity-dependent capacitance. The latter must give rise to a bilinear transformation mapping from the ε^* plane to the Γ^* plane, which would transform the $\varepsilon' = 1{\cdot}0$ contour to an arc of a circle (or a straight line) in the Γ^* plane.

The work described here has been carried out at the UK National Physical Laboratory as part of a programme to characterise a number of dielectric reference liquids in the radio and microwave frequency range. One of the aims of this work is to quantify and reduce measurement uncertainties by using a number of complementary methods, including liquid cell techniques. The numerical analyses described here are also being tested by measurements on the reference liquids, and the results of this experimental work will be reported elsewhere.

S. JENKINS
A. W. PREECE
Research Unit
Radiotherapy and Oncology Centre
Bristol BS2 8ED, United Kingdom

T. E. HODGETTS
Royal Signals and Radar Establishment
Malvern, Worcestershire WR14 3PS, United Kingdom

G. T. SYMM
A. G. P. WARHAM
R. N. CLARKE
National Physical Laboratory
Teddington, Middlesex TW11 0LW, United Kingdom

2nd January 1990

References

1 GRANT, J. P., CLARKE, R. N., SYMM, G. T., and SPYROU, N.: 'A critical study of the open-ended coaxial line sensor technique for RF and microwave complex permittivity measurements', *J. Phys. E, Sci. Instrum.*, 1989, **22**, pp. 757–770
2 MOSIG, J. R., BESSON, J. C. E., GEX-FABRY, M., and GARDIOL, F. E.: 'Reflection of an open-ended coaxial line and application to nondestructive measurement of materials', *IEEE Trans.*, 1981, **IM-30**, pp. 46–51
3 NEVELS, R. D., BUTLER, C. M., and YABLON, W.: 'The annular slot antenna in a lossy biological medium', *IEEE Trans.*, 1985, **MTT-30**, pp. 314–319
4 WARHAM, A. G. P.: 'Annular slot antenna radiating into lossy material'. National Physical Laboratory Report DITC 152/89, 1989
5 HODGETTS, T. E.: 'The open-ended coaxial line: a rigorous variational treatment'. Royal Signals and Radar Establishment Memorandum No. 4331, 1989
6 JORDAN, B. P., SHEPPARD, R. J., and SZWARNOWSKI, S.: 'The dielectric properties of formamide, ethanediol and methanol', *J. Phys. D, Appl. Phys.*, 1978, **11**, pp. 695–701

HIGH PERFORMANCE DFB-MQW LASERS AT 1·5 μm GROWN BY GSMBE

Indexing terms: Lasers and laser applications, Indium compounds, Gallium arsenide

1·5 μm GaInAs multiquantum well distributed feedback lasers have been successfully fabricated on InP grating substrate by GSMBE. DFB mode oscillation at high output power (50 mW) and narrow linewidth (1·3 MHz) have been obtained.

Introduction: Distributed feedback lasers with a quantum well active layer (DFB-MQW) emitting at 1·5 μm are very promising light sources for optical communications. They exhibit many advantages over the conventional double heterostructure due to the high differential gain and low spectral linewidth enhancement factor.[1] This results in narrow linewidth, low threshold current, high output power and high frequency response which is suitable for coherent transmission or high speed communication. High quality devices have been successfully obtained using metal organic vapour deposition (MOCVD) as the epitaxial technique.[2,3]

In this communication we report on DFB-MQW realised for the first time by gas source molecular beam epitaxy (GSMBE). We have demonstrated single mode operation up to 50 mW for long laser (1 mm) which is, to our knowledge, the best performance reported so far for DFB-MQW lasers. Narrow linewidth as low as 1·3 MHz has also been obtained on a 600 μm cavity length laser at 8 mW output power.